PNAS RESEARCH ARTICLE | DEVELOPMENTAL BIOLOGY

CHD7 and SOX2 act in a common gene regulatory network during mammalian semicircular canal and cochlear development

Jingxia Gao[a], Jennifer M. Skidmore[a], Jelka Cimerman[a], K. Elaine Ritter[a,1], Jingyun Qiu[b,c], Lindsey M. Q. Wilson[d], Yehoash Raphael[e], Kelvin Y. Kwan[b,c], and Donna M. Martin[a,f,2]

Edited by Janet Rossant, Gairdner Foundation, Toronto, ON, Canada; received July 29, 2023; accepted January 19, 2024

Inner ear morphogenesis requires tightly regulated epigenetic and transcriptional control of gene expression. CHD7, an ATP-dependent chromodomain helicase DNA-binding protein, and SOX2, an SRY-related HMG box pioneer transcription factor, are known to contribute to vestibular and auditory system development, but their genetic interactions in the ear have not been explored. Here, we analyzed inner ear development and the transcriptional regulatory landscapes in mice with variable dosages of *Chd7* and/or *Sox2*. We show that combined haploinsufficiency for *Chd7* and *Sox2* results in reduced otic cell proliferation, severe malformations of semicircular canals, and shortened cochleae with ectopic hair cells. Examination of mice with conditional, inducible *Chd7* loss by $Sox2^{CreER}$ reveals a critical period (~E9.5) of susceptibility in the inner ear to combined *Chd7* and *Sox2* loss. Data from genome-wide RNA-sequencing and CUT&Tag studies in the otocyst show that CHD7 regulates *Sox2* expression and acts early in a gene regulatory network to control expression of key otic patterning genes, including *Pax2* and *Otx2*. CHD7 and SOX2 directly bind independently and cooperatively at transcription start sites and enhancers to regulate otic progenitor cell gene expression. Together, our findings reveal essential roles for *Chd7* and *Sox2* in early inner ear development and may be applicable for syndromic and other forms of hearing or balance disorders.

ear development | epigenetics | CHARGE syndrome | cochlea | vestibular system

Significance

Little is known about the early molecular events that give rise to vestibular and auditory inner ear structures. We show that CHD7, a chromatin remodeler, and SOX2, a pioneer transcription factor, cooperate to help shape the inner ear. CHD7 regulates *Sox2* expression, and both genes bind near transcription start sites of key otic development and patterning genes, including *Pax2* and *Otx2*. We show that inner ear morphogenesis depends on proper dosage of both *Chd7* and *Sox2*. Our findings uncover a gene regulatory network that helps define the early epigenetic landscape of otic progenitor cells. These findings are relevant for understanding and treating hearing and balance disorders and shed light on potential interactions between these genes in other organs.

Genetic or environmental lesions that disrupt inner ear development cause auditory and/or vestibular dysfunction. Inner ear structures originate from the otic placode (op), a thickening of the surface ectoderm near the hindbrain, through a complex series of morphogenic events that convert the op to an otic cup, then a spherical otocyst, and ultimately into the mature inner ear. The dorsal inner ear vestibular organs include semicircular canals, utricle, and saccule, and their associated sensory structures are responsible for the perception of angular and linear movements. The organ of Corti, the cochlear sensory epithelium, is essential for sound perception. The organ of Corti is composed of one row of inner hair cells (IHCs) and three rows of outer HCs (OHCs) along with adjacent interdigitated supporting cells (SCs), including Deiters' cells (DCs), whose nuclei reside basal to the OHC bodies (1). Proper development of the inner ear requires highly orchestrated action by Wnt, Shh, Bmp, Fgf, and other morphogens (2–4), transcription factors (5), and planar cell polarity (PCP) proteins (6).

CHD7, Chromodomain Helicase DNA-binding Protein 7, is an epigenetic regulator and chromatin remodeler. *Chd7* is broadly expressed throughout the early developing otocyst and cochleovestibular ganglion (CVG) and is later localized to the vestibular and cochlear epithelia and associated spiral ganglion neurons (SGNs) (7). Haploinsufficiency of human *CHD7* causes CHARGE syndrome, a multiple anomaly condition characterized by ocular coloboma, heart defects, atresia of the choanae, retarded growth and development, genital hypoplasia, and ear defects, including deafness and semicircular canal dysgenesis (8). Mice with heterozygous loss of *Chd7* exhibit hypoplasia/dysplasia of posterior and lateral semicircular canals, abnormal innervation in the vestibular sensory epithelium (9), and reduced neuroblast proliferation (10). *Chd7* heterozygous mutant mice exhibit mixed conductive and sensorineural hearing loss despite intact auditory sensory epithelia and associated innervation (11, 12). Conditional deletion of *Chd7* using a pan-otic *Cre* leads to hypoplasia of semicircular canals and disorganized innervation of the organ of Corti (10, 13). Thus, *Chd7* has pleiotropic roles in early development of auditory and vestibular structures.

SOX2 (HMG-box transcription factor sex-determining region Y-box 2) belongs to the group B family of SOX transcription factors and is one of the earliest genes to mark neurosensory progenitors in the otic epithelium. *Sox2* is expressed in the lateral edge of the op as early as E8.5 in mice (14) and subsequently expands into the dorsal domain, marking presumptive anterior and lateral cristae and utricle, and into the ventral domain,

Author contributions: J.G., J.M.S., K.E.R., Y.R., K.Y.K., and D.M.M. designed research; J.G., J.M.S., J.C., and K.E.R. performed research; J.G., J.M.S., K.E.R., J.Q., L.M.Q.W., K.Y.K., and D.M.M. analyzed data; and J.G., J.M.S., J.C., K.E.R., J.Q., Y.R., K.Y.K., and D.M.M. wrote the paper.

The authors declare no competing interest.

This article is a PNAS Direct Submission.

[1]Present address: Division of Molecular Oncology, Department of Oncology, St. Jude Children's Research Hospital, Memphis, TN 38105.

[2]To whom correspondence may be addressed. Email: donnamm@umich.edu.

This article contains supporting information online at https://www.pnas.org/lookup/suppl/doi:10.1073/pnas.2311720121/-/DCSupplemental.

Published February 26, 2024.

which gives rise to the organ of Corti and saccule (15). *Sox2* expression persists postnatally in differentiated SCs and SGNs (16). Mice with complete loss of *Sox2* in the ear (*Lcc/Lcc*) fail to establish a prosensory domain, resulting in the absence of HCs and SCs (17). *Sox2* also regulates the expansion of neurosensory progenitor cells and initiates differentiation of HCs by binding and activating *Atoh1*, a transcription factor essential for HC differentiation (18). Conditional deletion of *Sox2* in the developing otocyst leads to neurogenesis defects and premature death of neurosensory progenitors (19). In addition, *Sox2*-expressing cells in the early otocyst give rise to large numbers of nonsensory structures throughout the inner ear (20), and early *Sox2* loss impairs formation of nonsensory structures including semicircular canals and vestibular maculae (21).

CHD7 has been shown to bind to thousands of sites in the vertebrate genome and is enriched at enhancers and transcription start sites (TSSs) (22). In neural stem cells, SOX2 and CHD7 physically interact, bind to overlapping sites in the genome, and regulate a set of common target genes including *Jag1*, *Gli3,* and *Mycn* (23). SOX2 also collaborates with CHD7 to regulate the expression of *regulator of cell cycle* (*Rgcc*) and *protein kinase C-θ* (*PKCθ*) to activate oligodendrocyte precursor cells after spinal cord injury (24). Previous studies showed reduced *Sox2* inner ear expression in *Chd7* conditional knockout mice (25), suggesting that CHD7 and SOX2 act in a common genetic pathway and have overlapping or complementary functions during inner ear development.

Here, using mice with germline or conditional inducible deletions, we tested the hypothesis that a *Chd7-Sox2* gene regulatory network functions to promote prosensory and sensory cell development in the ear. Our results show that CHD7 and SOX2 cooperate to regulate morphogenesis of the semicircular canals and the cochlea, via effects on cell proliferation and regulation of other developmentally critical genes. Genome-wide analysis shows that *Chd7* acts upstream of *Sox2* and regulates a broad set of target genes. CHD7 and SOX2 bind to unique and common regions of the genome, including near TSSs and/or enhancers of genes that are critical for inner ear formation and patterning. These studies provide a basis for understanding combined functions of *Chd7* and *Sox2* in the inner ear and help define the early otic transcriptional regulatory landscape.

Results

CHD7 and SOX2 Expression and Hierarchy during Inner Ear Development. *Chd7* and *Sox2* are highly expressed in the developing mouse otocyst and play important roles in proneurosensory development (10, 17). Prior studies showed *Chd7* expression at E8.5 in the neural tube (26) and in the E9.5 otocyst (27) and *Sox2* expression in the proneural region of the E9.5 otocyst (15). To determine the precise timing of *Chd7* and *Sox2* coexpression in the developing ear, we performed double immunofluorescence on sectioned inner ears from E8.5-E11.5 wild-type (WT) embryos (Fig. 1). *Chd7* and *Sox2* were both expressed throughout the neural tube and op at E8.5 (Fig. 1 *A–C*). Over the next 2 d of embryonic development, CHD7 and SOX2 were enriched in the ventral otocyst and cochleovestibular and facial ganglia (E9.5-E10.5). Notably, *Chd7* expression was broader than *Sox2* in both otocyst and ganglia (Fig. 1 *D–I*). By E11.5, CHD7 and SOX2 were enriched in the ventral otocyst, and CHD7 was abundant in the CVG, whereas SOX2 was present in both the cochleovestibular and facial ganglion (Fig. 1 *J–L*). Given their complex expression patterns, we asked whether CHD7 and

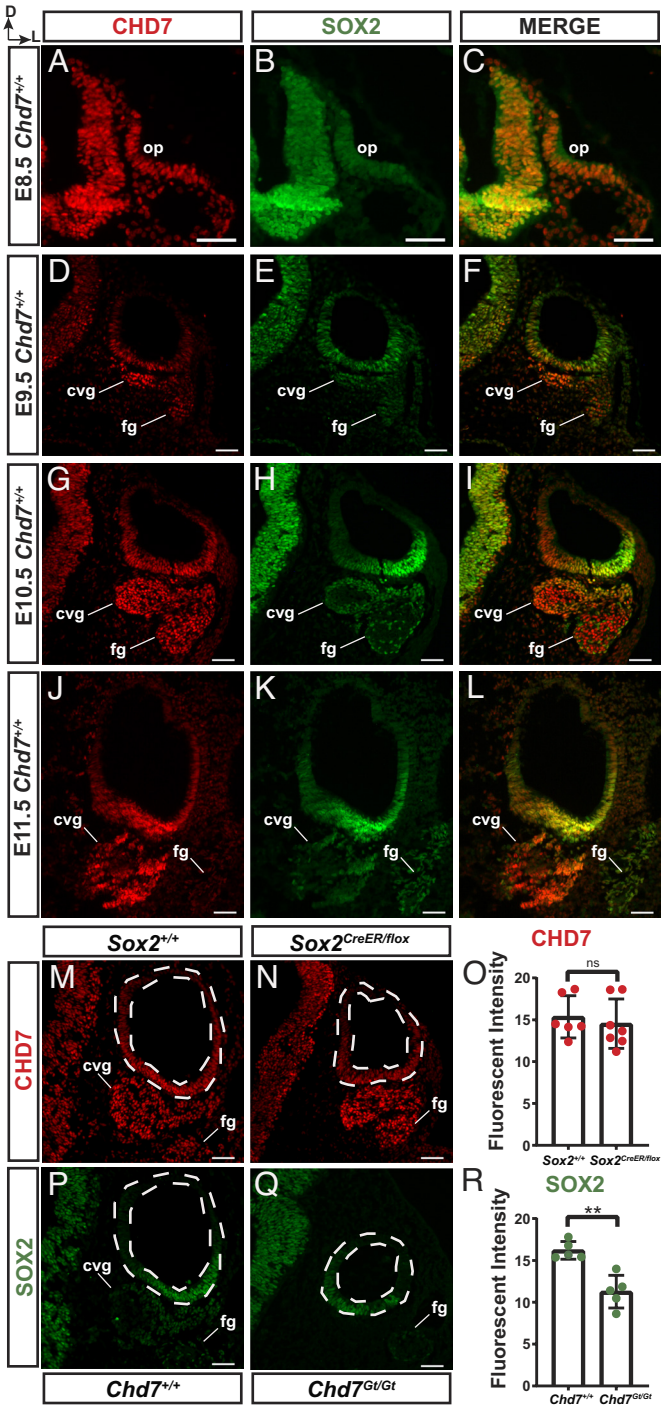

Fig. 1. CHD7 colocalizes with and regulates *Sox2* expression in the otocyst. (*A–L*) Transverse sections from E8.5-E11.5 WT embryos costained with anti-CHD7 (red) and anti-SOX2 (green). Dorsal is up and lateral is right for all sections. At E8.5, CHD7 and SOX2 broadly colocalize in the neural tube and op (*A–C*). At E9.5, CHD7 and SOX2 are both present in the ventral otocyst and cvg while CHD7 is also present in the facial ganglion (fg) (*D–F*). At E10.5, CHD7 and SOX2 are enriched in the ventrolateral otocyst; in the cvg and fg; CHD7 is present in a broader region than SOX2 (*G–I*). At E11.5, double positive (CHD7+/SOX2+) cells are abundant in the ventral otocyst while the cvg and the fg contain primarily singly labeled CHD7+ or SOX2+ cells, respectively (*J–L*). (*M* and *N*) E10.5 transverse sections from WT and $Sox2^{CreER/flox}$ embryos treated with tamoxifen/progesterone at E8.5, E9.5, and E10 and stained with anti-CHD7. (*O*) Quantification of CHD7 immunofluorescence showed no difference between $Sox2^{+/flox}$ control and $Sox2^{CreER/flox}$ otocysts ($n = 5$ per genotype). (*P* and *Q*) E10.5 transverse sections from WT or $Chd7^{Gt/Gt}$ embryos stained with anti-SOX2. (*R*) Quantification of SOX2 immunofluorescence showed a ~30% decrease in $Chd7^{Gt/Gt}$ otocysts compared to WT ($n = 5$ per genotype). Dashed lines in (*M*, *N*, *P*, and *Q*) denote the otic vesicle. ***$P < 0.01$. (Scale bar, 50 μm.)

SOX2 participate in the same or distinct gene regulatory networks of the inner ear by assaying *Chd7* expression in the absence of *Sox2* and vice versa. To avoid the embryonic lethality of complete *Sox2* deficiency (28), we induced *Sox2* deletion in $Sox2^{CreER/flox}$ embryos, in which one *Sox2* allele contains a CreER fusion protein in place of the coding region, and the other allele has *loxP* sites flanking the coding region (29). *Sox2* was deleted by maternal intraperitoneal injection of tamoxifen at E8.5, E9.5, and E10, followed by harvesting embryos at E10.5. SOX2 immunostaining of otocyst sections at E10.5 showed that *Sox2* expression was severely diminished in $Sox2^{CreER/flox}$ otocysts compared to $Sox2^{+/flox}$ (*SI Appendix*, Fig. S1 *A* and *B*). CHD7 immunofluorescence in the otocyst was unchanged in $Sox2^{CreER/flox}$ embryos compared to $Sox2^{+/flox}$littermates (n = 5 ears; Fig. 1 *M–O*). By contrast, SOX2 immunofluorescence was reduced ~30% in $Chd7^{Gt/Gt}$ otocysts compared to WT (n = 5 ears, $P < 0.01$; Fig. 1 *P–R*) (the $Chd7^{Gt}$ allele expresses a gene trapped β-geo construct, resulting in a null allele) (27). These studies confirm that *Chd7* is genetically upstream of *Sox2* in otic development.

Chd7 and Sox2 Genetically Interact during a Critical Window of Inner Ear Development. *Chd7* loss results in highly penetrant semicircular canal defects that are detectable as early as E12.5 (10, 27). *Sox2* is also required between E8.5 and E10.5 for semicircular canal formation (17, 21). Previous studies showed that CHD7 and SOX2 physically interact in brain-derived mouse neural stem cells (23), but whether these genes function cooperatively in the ear is unknown. To test this, we crossed $Sox2^{CreER}$ and $Chd7^{flox}$ alleles and induced Cre-mediated deletion at E8.5, E9.5, or E10.5 and assessed E14.5 inner ears by paint-fill. Since $Sox2^{CreER/+}$ mice have only one functional copy of *Sox2*, this cross provides insights into the timing of interactions between *Sox2* and *Chd7* as well as temporal requirements for *Chd7* during inner ear development. After tamoxifen exposure at E8.5, E14.5 control ($Chd7^{flox/flox}$ or $Chd7^{flox/+}$) and $Sox2^{CreER/+};Chd7^{flox/+}$ ears exhibited normal morphology (Fig. 2*A*; n = 12 and Fig. 2*B*; n = 20, respectively), whereas $Sox2^{CreER/+};Chd7^{flox/flox}$ ears displayed malformed lateral semicircular canals (n = 2 of 6 ears) (Fig. 2*C* and *SI Appendix*, Fig. S2 *H* and *L* and Table S3). Interestingly, tamoxifen treatment of $Sox2^{CreER/+};Chd7^{flox/+}$ears at E9.5 led to severely malformed lateral semicircular canals (n = 5 of 6 ears) (Fig. 2*E* and *SI Appendix*, Fig. S2 *A–F* and Table S3). Among $Sox2^{CreER/+};Chd7^{flox/flox}$ ears treated with tamoxifen at E9.5, all (n = 6 of 6 ears) lateral semicircular canals were aplastic or hypoplastic, and posterior semicircular canals were truncated (n = 2 of 6 ears) (Fig. 2*F* and *SI Appendix*, Fig. S2 *M–R* and Table S3). Tamoxifen treatment at E10.5 (Fig. 2 *G–I* and *SI Appendix*, Fig. S2 *S–X* and Table S3) resulted in low penetrance (n = 1 of 6 ears) lateral canal hypoplasia in E14.5 $Sox2^{CreER/+};Chd7^{flox/flox}$ embryos and normal inner ears in $Chd7^{flox/flox}$ (n = 6 of 6 ears) and $Sox2^{CreER/+};Chd7^{flox/+}$ (n = 6 of 6 ears) embryos. Together, these results indicate that the period around E9.5 is critical in mice for *Chd7* function and genetic interactions between *Sox2* and *Chd7* that help shape the inner ear.

Double Haploinsufficiency of Chd7 and Sox2 Leads to Vestibular Defects and Shortened Cochleae with Decreased Cell Proliferation. Previous studies have shown that *Chd7* is critical for embryonic viability since homozygous null ($Chd7^{Gt/Gt}$) embryos do not survive beyond E10.5 (7, 27). In contrast, heterozygous loss of *Chd7* ($Chd7^{Gt/+}$) results in mice that do survive after birth but exhibit circling behavior, cleft palate, growth delay, and feeding difficulties and variably reduced postnatal survival (27). Single-copy loss of *Sox2* does not impact overall survival or inner ear development (29, 30). To further test for functional interactions,

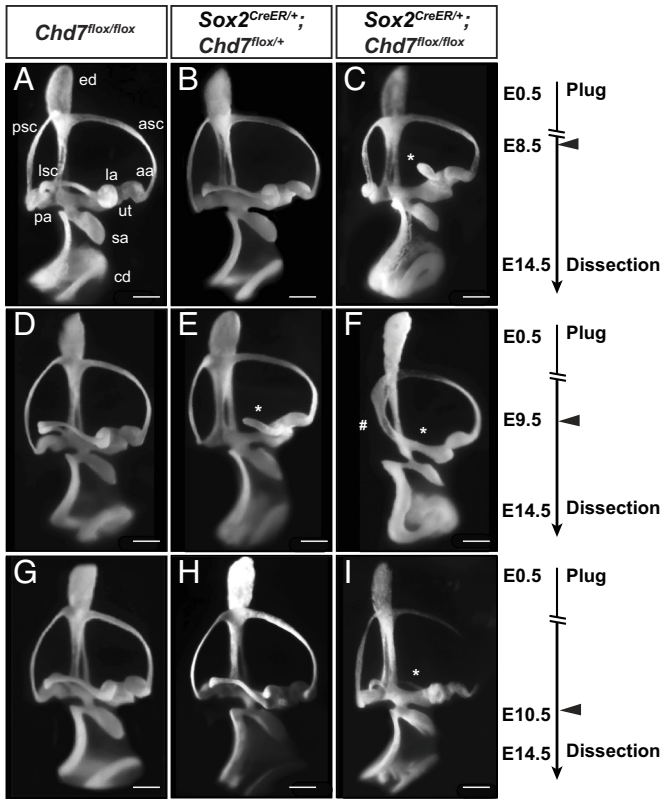

Fig. 2. *Chd7* and *Sox2* genetically interact during a critical period of inner ear development. Paint-filled E14.5 inner ears from crosses between $Sox2^{CreER}$ and $Chd7^{flox/flox}$ mice after tamoxifen induction at E8.5 (*A–C*), E9.5 (*D–F*), or E10.5 (*G–I*). Conditional heterozygous embryos exhibited dysplastic lateral semicircular canals (*) after *Cre* induction at E9.5 (n = 5 of 6 ears; *E*) but not at E8.5 or E10.5 (*B* and *H*). In contrast, conditional knockout embryos exhibited dysplastic lateral semicircular canals after tamoxifen treatment at E8.5 (n = 2 of 6 ears), E9.5 (n = 6 of 6 ears), or E10.5 (n = 1 of 6 ears) and hypoplastic or truncated posterior semicircular canals (#) after tamoxifen treatment at E9.5 (n = 2 of 6 ears; *F*) but not at E8.5 or E10.5. Abbreviations: aa, anterior ampulla; asc, anterior semicircular canal; cd, cochlear duct; ed, endolymphatic duct; la, lateral ampulla; lsc, lateral semicircular canal; pa, posterior ampulla; psc, posterior semicircular canal; sa, saccule; ut, utricle. All ears are shown in lateral view. (Scale bar, 50 μm.)

we generated mice with heterozygous deletions of both *Chd7* ($Chd7^{Gt/+}$) and *Sox2* ($Sox2^{CreER/+}$). Mice were observed on the day of birth (P0) and each subsequent day for 6 d (*SI Appendix*, Fig. S3 *A* and *B* and Table S2). Survival of $Chd7^{Gt/+}$ mice was lower ($P < 0.05$) than WT or $Sox2^{CreER/+}$ mice at P6, and survival of $Chd7^{Gt/+};Sox2^{CreER/+}$ mice was significantly reduced compared to WT, $Sox2^{CreER/+}$ ($P < 0.0001$), or $Chd7^{Gt/+}$ ($P < 0.01$, log-rank test) mice. Eight of 14 $Chd7^{Gt/+};Sox2^{CreER/+}$ mice died on the day of birth, another four died by P1, and only two mice survived the entire 6-d observation period. The cause of death is unknown, but *Chd7* and *Sox2* also exhibit overlapping expression in the developing brain, heart, and craniofacial structures, and functional cooperativity in these organs may be a contributing factor. These results demonstrate that *Chd7* and *Sox2* act together to promote critical aspects of mammalian development.

$Chd7^{Gt/+}$ mice exhibit highly penetrant inner ear defects of the lateral and posterior semicircular canals and associated cristae (9, 10, 25), whereas $Sox2^{CreER/+}$ mice have normal inner ear membranous labyrinths (21). Loss of two alleles of *Chd7* or *Sox2* (in conditional nulls) results in severely malformed vestibular and auditory structures (10, 21). In our study, paint-filled membranous labyrinths from E14.5 WT (Fig. 3*A*, n = 12) and $Sox2^{CreER/+}$ embryos (Fig. 3*C*, n = 4) showed normal inner ear morphology, whereas $Chd7^{Gt/+}$ mice exhibited the typical dysplasia of posterior

and lateral semicircular canals (Fig. 3*B*, $n = 12$) (9, 10). Strikingly, $Chd7^{Gt/+};Sox2^{CreER/+}$ inner ears displayed almost complete aplasia of the lateral and anterior semicircular canals, dysplasia of the posterior semicircular canal, malformed endolymphatic duct, absence of anterior, lateral, and posterior ampullae, absence of the utricle, and shortened saccule; in addition, the cochlea was undercoiled (Fig. 3*D*, $n = 7$). The inner ear abnormalities in double heterozygous *Chd7* and *Sox2* embryos bore a striking resemblance to those from *Chd7* conditional knockout or *Sox2* null mice.

To better understand the auditory defects in *Chd7;Sox2* double heterozygous mutant mice, we examined the cochleae at P0, the latest time at which we could recover adequate tissues. Cochlear length at P0 was similar in WT (Fig. 3 *E* and *I*, 4,970±57 μm, $n = 6$ ears), $Chd7^{Gt/+}$ (Fig. 3 *F* and *I*, 4,442 ± 55 μm, $n = 8$ ears, $P = 0.19$), and $Sox2^{CreER/+}$ (Fig. 3 *G* and *I*, 4,740 ± 80 μm, $n = 8$ ears, $P = 0.99$, one-way ANOVA) mice. In contrast, cochlear length was 39.4% reduced in $Chd7^{Gt/+};Sox2^{CreER/+}$ mice (Fig. 3 *H* and *I*, 2,901 ± 189 μm, $P < 0.0001$; $n = 12$ ears, one-way ANOVA) compared to WT littermates. We further examined the membranous labyrinth in E18.5 inner ear transverse sections stained with hematoxylin and eosin. $Chd7^{Gt/+};Sox2^{CreER/+}$ embryos exhibited smaller inner ear capsules and fewer cochlear turns compared to WT littermates (Fig. 3 *J* and *K*); however, the cross-sectional appearance of the cochlear fluid spaces (scala vestibuli, scala media, and scala tympani) was normal, as were Reissner's membrane and the stria vascularis (Fig. 3 *J'* and *K'*).

Since regulation of cellular apoptosis, proliferation, and cell cycle exit (CCE) are all essential for proper cochlear development, we sought to determine whether any of these biological processes were disrupted upon loss of *Chd7* and *Sox2*. Anti-cleaved Caspase-3 was used to detect apoptotic cells. We observed similar anti-cleaved Caspase-3 immunostaining in the endolymphatic duct and ventralmost region of E10.5 WT and $Chd7^{Gt/+};Sox2^{CreER/+}$ otocysts (*SI Appendix*, Fig. S3 *C–H*, arrows and arrowheads, respectively). There were no apoptotic cells detected in either $Chd7^{Gt/+};Sox2^{CreER/+}$ or WT cochlear region at E11.5, consistent with a previous report on cell death in the WT ear (31). To determine whether the shortened cochlea was caused by premature CCE of prosensory cells, we injected pregnant females with the thymidine analog 5-ethynyl-2′-deoxyuridine (EdU) at E13.5 or E12.5, harvested cochleae at P0 and labeled HCs with anti-Myo7a antibody. EdU+ OHCs at the time of harvest were interpreted as having arisen from mitotic precursors at the time of injection. Reduced numbers of EdU+ HCs indicate premature CCE, whereas increased number of EdU+ HCs indicates delayed CCE. $Chd7^{Gt/+};Sox2^{CreER/+}$ and WT cochleae exposed to EdU at E13.5 both showed the typical apical to basal gradient of EdU staining (CCE) (32) (*SI Appendix*, Fig. S3*I*), whereas $Chd7^{Gt/+};Sox2^{CreER/+}$ cochleae exposed to EdU at E12.5 showed minimal premature CCE in the middle and delayed CCE in the base of the cochleae (*SI Appendix*, Fig. S3*J*). To assay for changes in cell proliferation, we used anti-phospho-Histone H3 (pHH3), which marks cells in mitosis. In contrast to normal apoptosis and minimally changed CCE, anti-pHH3 immunofluorescence was reduced by 27% in $Chd7^{Gt/+};Sox2^{CreER/+}$ E10.5 otocysts and by 32.1% at E11.5 compared to WT (Fig. 3 *L–P*). The lack of major changes in CCE at E12.5 and E13.5 in $Chd7^{Gt/+};Sox2^{CreER/+}$ cochleae also suggests that cell proliferation is normal at these stages. From these experiments, we conclude that cell proliferation, but not CCE or apoptosis, is highly sensitive to combined loss of *Chd7* and *Sox2*.

Chd7 and Sox2 Cooperate to Promote Cochlear Epithelial Organization. The significantly shortened cochleae in $Chd7^{Gt/+};Sox2^{CreER/+}$ mice prompted us to examine cochlear epithelial and cellular structures. Previous studies showed that *Chd7* is expressed in mature cochlear HCs (11) whereas *Sox2* is expressed in early postnatal cochlear SCs (33). Given the extensive colocalization of these two proteins in early ear development, we asked when their expression in the sensory epithelium diverges. At E14.5, *Chd7* was broadly expressed in the cochlear floor, including (but not restricted to) the SOX2 positive prosensory domain (Fig. 4 *A–C*). At E18.5, around the time that IHCs and OHCs are identifiable, *Chd7* remained broadly expressed in the cochlear floor, including in both HCs and SCs, whereas *Sox2* was still expressed in HCs but highly expressed in SCs (Fig. 4 *D–F*), which is consistent with published data (18).

Prior studies have shown that cochlear anatomy is normal in $Chd7^{Gt/+}$ mice (11), whereas conditional deletion of *Chd7* leads to abnormal innervation and organization of the cochlear epithelium (11, 13). *Sox2* heterozygous loss results in supernumerary IHCs (30). We examined the HCs of the cochlea in all four genotypes (WT, $Chd7^{Gt/+}$, $Sox2^{CreER/+}$, and $Chd7^{Gt/+};Sox2^{CreER/+}$) by staining P0 whole-mounted cochleae with the hair cell marker Myosin7a (Myo7a). In WT ($n = 4$ ears) and $Chd7^{Gt/+}$ ($n = 4$ ears) cochlear epithelia, anti-Myo7a labeled the typical three rows of OHCs and one row of IHCs with occasional supernumerary HCs primarily present in the apex and middle regions (Fig. 4 *G1–G3* and *H1–H3*). As expected, $Sox2^{CreER/+}$ ($n = 3$ ears) cochleae exhibited occasional supernumerary IHCs located at the neural side of the single row of IHCs (Fig. 4 *I1–I3*) (30, 34). The number of supernumerary IHCs (1.6 ± 0.6/100 μm, $n = 5$ cochleae) in the apical turn was significantly higher in $Sox2^{CreER/+}$ cochleae compared to WT ($P < 0.05$, two-way ANOVA) or $Chd7^{Gt/+}$ cochleae ($P < 0.05$, Fig. 4*K*). In $Chd7^{Gt/+};Sox2^{CreER/+}$ cochleae, the number of supernumerary IHCs in all three cochlear turns (base, middle, and apex) was comparable to those in the corresponding turns in $Sox2^{CreER/+}$ cochleae (Fig. 4*K*), suggesting that *Sox2* regulates IHC number throughout the organ of Corti. No supernumerary OHCs were present in WT, $Chd7^{Gt/+}$ or $Sox2^{CreER/+}$ cochleae (Fig. 4 *G1–I3*), whereas abundant supernumerary OHCs were observed in the basal and middle turns of $Chd7^{Gt/+};Sox2^{CreER/+}$ cochleae (Fig. 4 *J1–J3*, arrows). Notably, one additional row of supernumerary OHCs was present in the apical turn of $Sox2^{CreER/+};Chd7^{Gt/+}$ cochleae (Fig. 4*J3*, arrow). The number of supernumerary OHCs in $Chd7^{Gt/+};Sox2^{CreER/+}$ cochleae was significantly higher in the middle turn (5.1 ± 1.5/100 μm, $P < 0.05$) and apical turn (8.8 ± 1.5/100 μm, $P < 0.0001$) in comparison to cochleae from all three other genotypes (Fig. 4*L*). These results indicate that supernumerary OHCs occur in $Chd7^{Gt/+};Sox2^{CreER/+}$ cochleae in a graded manner with the most severe phenotypes in the apex and the least severe in the base.

Severe cochlear hypoplasia and supernumerary OHCs in $Chd7^{Gt/+};Sox2^{CreER/+}$ mice prompted us to ask whether cochlear innervation might also depend on proper dosage of *Chd7* and *Sox2*. Prior studies showed that single-copy *Chd7* loss does not impact cochlear innervation, while two-copy loss due to deletion with $Foxg1^{Cre/+}$, *Pax2Cre*, or *Ngn1Cre* results in severely misguided cochlear neurites (13). *Sox2* regulates neurogenesis in the inner ear in a dosage-dependent manner (19) and is critical for hair cell development (17, 21); mice with heterozygous loss of *Sox2* show normal hearing (30), and no innervation defects have been reported. To assess cochlear innervation, we applied the neurite marker anti-neurofilament (NF) to P0 whole-mounted cochleae to detect neurites projected from SGNs that synapse on IHCs or pass through the IHC region to synapse on OHCs. In the region of OHCs, neurite projections typically arc toward the basal region of the cochlea, with multiple neurites gathering beneath each row of OHCs to form outer spiral bundles (Fig. 4 *G1'–J2'*). These outer spiral bundles are still immature in the apical turn of the cochleae at early postnatal stages (Fig. 4 *G3'–J3'*) since the development of SGNs and neurites in the cochleae begins in the basal turn and

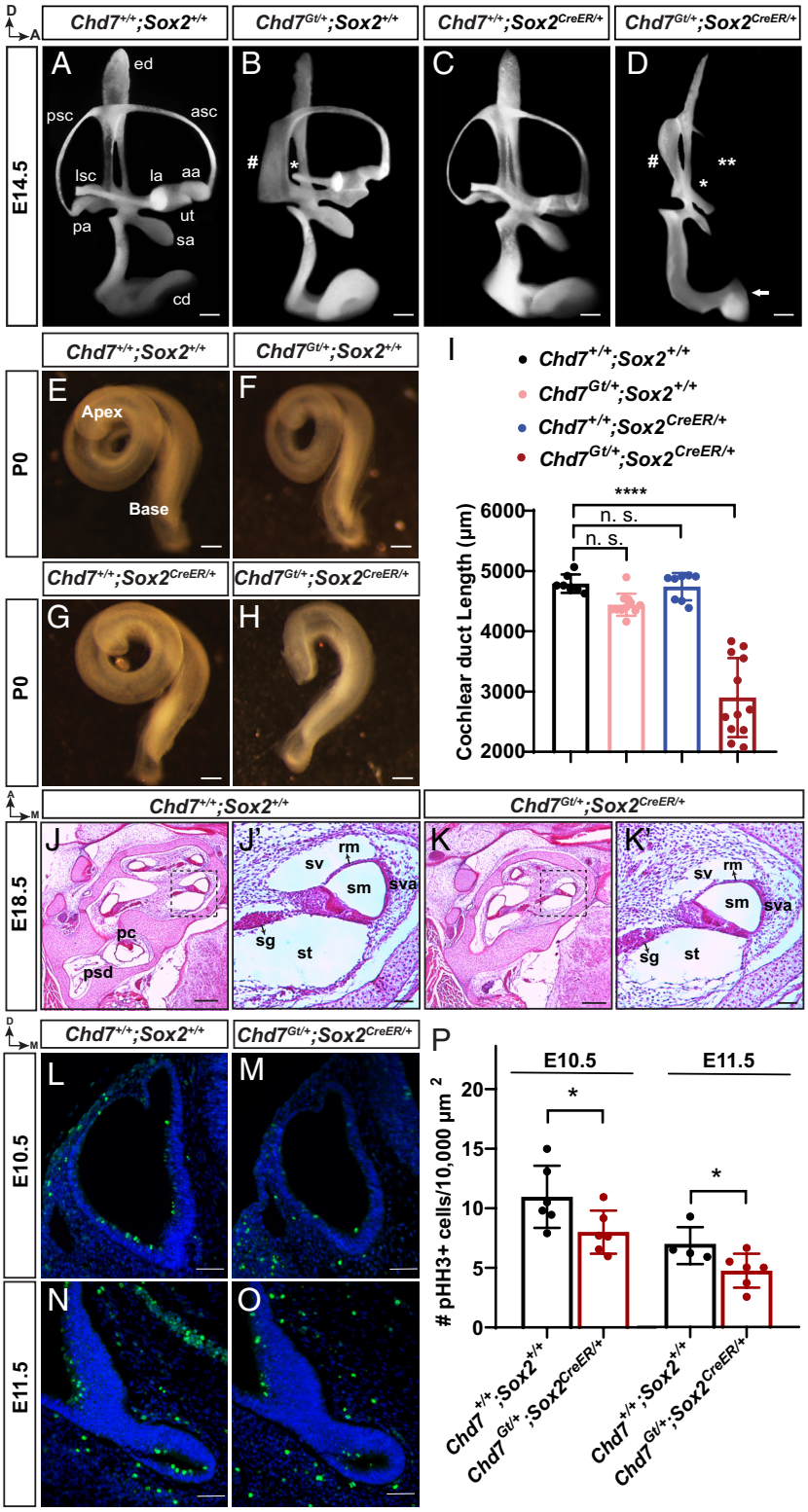

Fig. 3. Mice with heterozygous deletion of *Chd7* and *Sox2* exhibit vestibular defects and shortened cochleae with decreased cell proliferation. (*A–D*) Paint-filled membranous labyrinths of E14.5 WT (*A*, *n* = 12) and $Sox2^{CreER/+}$ (*C*, *n* = 4) mice show normal inner ear morphology, whereas $Chd7^{Gt/+}$ ears (*B*, *n* = 12) show dysplasia of posterior (#) and lateral (*) semicircular canals; $Chd7^{Gt/+};Sox2^{CreER/+}$ ears (*D*, *n* = 7) exhibit almost complete loss of lateral (*), anterior (**), and posterior (#) semicircular canals along with malformed endolymphatic duct, absent ampullae and utricle, shortened saccule, and hypoplastic cochlear duct (arrow). (*E–H*) Representative bright field images of whole-mounted cochleae from P0 WT (*E*), $Chd7^{Gt/+}$ (*F*), $Sox2^{CreER/+}$ (*G*), and $Chd7^{Gt/+};Sox2^{CreER/+}$ (*H*) mice. (*I*) Bar graph showing reduced cochlear length in double heterozygous $Chd7^{Gt/+};Sox2^{CreER/+}$ mice compared to WT. n.s., not significant; ****$P < 0.0001$, log-rank test. (*J–K'*) Representative bright field images of hematoxylin and eosin stained E18.5 transverse sections through the inner ear from WT (*J* and *J'*) and $Chd7^{Gt/+};Sox2^{CreER/+}$ (*K* and *K'*) mice. *J'* and *K'* depict magnified images of the *Inset* panels from (*J* and *K*). (*L–O*) Anti-phospho-Histone H3 and DAPI counterstaining of transverse sections through the otocyst from E10.5 (*L* and *M*) or E11.5 (*N* and *O*), $Chd7^{+/+};Sox2^{+/+}$ (*L* and *N*) or $Chd7^{Gt/+};Sox2^{CreER/+}$ (*M* and *O*) embryos. (*P*) Quantitation of phospho-Histone H3-positive cells in the otocyst at E10.5 and cochlear region at E11.5 from $Chd7^{Gt/+};Sox2^{CreER/+}$ (red) embryos and $Chd7^{+/+};Sox2^{+/+}$ (black) littermate embryos. *n* = 5 for each group. Abbreviations: pa, posterior ampulla; psd, posterior semicircular duct; rm, Reissner's membrane; sg, spiral ganglion; sm, scala media; st, scala tympani; sv, scala vestibuli; sva: stria vascularis. *$P < 0.05$, Student's *t* test. [Scale bar, 150 µm in (*J* and *K*); Scale bar, 50 µm in other images.]

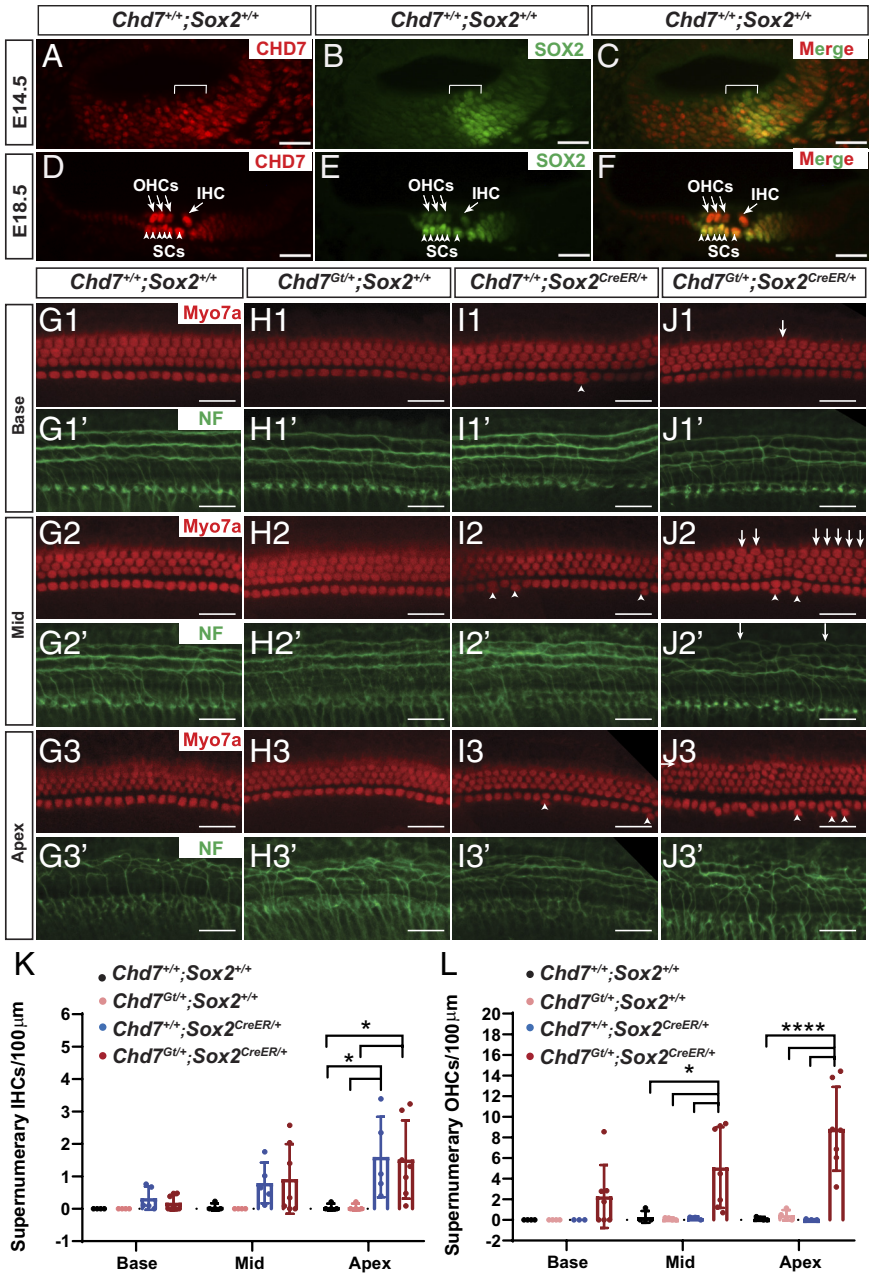

Fig. 4. *Chd7* and *Sox2* cooperate to establish proper hair cell numbers. WT cochleae from E14.5 (*A*–*C*) and E18.5 (*D*–*F*) embryos stained with anti-CHD7 (*A* and *D*) and anti-SOX2 (*B* and *E*). CHD7 is present in a broad cochlea region whereas SOX2 is restricted to the prosensory domain (brackets in *A*–*C*) at E14.5. At E18.5, CHD7 is abundant in IHCs and OHCs HCs (arrows) and SCs (arrowheads) while SOX2 is lower in HCs and enriched in SCs. (*G1*–*J3*′) Representative images of whole-mounted organ of Corti immunostained with anti-Myo7a (*G1*–*J1*, *G2*–*J2*, and *G3*–*J3*) and anti-NF (*G1*′–*J1*′, *G2*′–*J2*′, and *G3*′–*J3*′) in the basal (*G1*–*J1*′), middle (*G2*–*J2*′), and apical (*G3*–*J3*′) turns of WT (*G1*–*G3*′), $Chd7^{Gt/+}$ (*H1*–*H3*′), $Sox2^{CreER/+}$ (*I1*–*I3*′), and $Chd7^{Gt/+}$;$Sox2^{CreER/+}$ (*J1*–*J3*′) cochleae. Supernumerary OHCs are present in $Chd7^{Gt/+}$;$Sox2^{CreER/+}$ cochlea in both basal and middle turns (arrows in *J1* and *J2*), whereas an additional row of OHCs is present in the apex (arrow in *J3*). Supernumerary IHCs in $Sox2^{CreER/+}$ and $Chd7^{Gt/+}$;$Sox2^{CreER/+}$ cochleae are indicated by arrowheads (*I1*, *I2*, *I3*, *J2*, and *J3*). NF staining shows normally organized neurite projections in all genotypes. Ectopic neurites project to supernumerary OHCs in the middle turn of the $Chd7^{Gt/+}$;$Sox2^{CreER/+}$ cochlea (arrows in *J2*′). (*K*) Quantification of supernumerary IHCs shows a significant increase in the number of IHCs solely in the apical turn for both $Sox2^{CreER/+}$ and $Chd7^{Gt/+}$;$Sox2^{CreER/+}$ cochleae compared to WTor $Chd7^{Gt/+}$;$Sox2^{+/+}$ cochleae. (*L*) Quantification of supernumerary OHCs shows significant increase in supernumerary OHCs in the middle and apical turns, but not in the basal turn in $Chd7^{Gt/+}$;$Sox2^{CreER/+}$ cochleae compared to all three other genotypes. In (*K* and *L*), *$P < 0.05$, ****$P < 0.0001$, one-way ANOVA. [Scale bar, 50 µm in (*A*–*F*) and 25 µm in (*G1*–*J3*).]

progresses toward the apical turn (35). Cochlear innervation in P0 $Chd7^{Gt/+}$ (Fig. 4 *H1*′–*H3*′) and $Sox2^{CreER/+}$ (Fig. 4 *I1*′–*I3*′) mice appeared similar to WT (Fig. 4 *G1*′–*G3*′). In addition, cochlear innervation in $Chd7^{Gt/+}$;$Sox2^{CreER/+}$ mice (Fig. 4 *J1*′–*J3*′) appeared normal, except that ectopic outer spiral bundles were present in association with supernumerary OHCs (Fig. 4*J2*′). These results indicate that single-copy loss of *Chd7* and/or *Sox2* is not sufficient to disrupt cochlear innervation and that supernumerary OHCs of the double heterozygous mutant receive neurite innervation from their associated SGNs.

Since HCs and SCs arise from common progenitor cells, defects that give rise to changes in the number or integrity of HCs might also disrupt the number of SCs. Loss or reduction of the Notch signaling genes *Dll1*, *Jagged2*, or *Notch1* in mice leads to supernumerary HCs at the expense of SCs (36). To determine whether the supernumerary OHCs observed in $Chd7^{Gt/+}$;$Sox2^{CreER/+}$

cochleae were associated with changes in the number of SCs, we examined the cellular structure of the organ of Corti. In WT mice, phalloidin labeled the stereociliary bundle located on one side of HCs (*SI Appendix*, Fig. S4*A1*), whereas Prox1 antibody labeled inner pillar cells, outer pillar cells, and three rows of DCs at early postnatal stages (*SI Appendix*, Fig. S4*A1'*) (37). Supernumerary Prox1-positive SCs were observed in the middle turn of $Chd7^{Gt/+};Sox2^{CreER/+}$ cochleae, in the same region of the cochlea where supernumerary OHCs were present (*SI Appendix*, Fig. S4 *D2'* and *D2*, respectively, dots). In the apical turn, where one additional row of OHCs was identified (*SI Appendix*, Fig. S4*D3*, arrow), an additional row of Prox1-labeled SCs was also present (*SI Appendix*, Fig. S4*D3'*, arrow). These results demonstrate that in $Chd7^{Gt/+};Sox2^{CreER/+}$ cochleae, supernumerary SCs are present in areas of the cochleae where supernumerary OHCs are also found, suggesting that supernumerary OHCs production does not occur at the expense of nearby SCs.

Previous studies have demonstrated the importance of the PCP signaling pathway in cochlear development. Mice with mutations in various members of the PCP pathway display shortened cochleae, and some also exhibit disrupted stereociliary bundle orientation (6). To determine whether *Chd7* and *Sox2* functionally interact to regulate PCP signaling, we analyzed bundle orientation in cochleae from mice of all four genotypes (WT, $Chd7^{Gt/+}$, $Sox2^{CreER/+}$, and $Chd7^{Gt/+};Sox2^{CreER/+}$). The cartoon in *SI Appendix*, Fig. S4*E* (adapted from ref. 38) illustrates the method used to measure bundle orientation. Specifically, the orientation of individual stereociliary bundles was scored as 0° when the line drawn from the vertex through the symmetric bundle ran parallel to the neural-abneural axis. When the bundle was rotated clockwise (or counterclockwise), bundle orientation was scored as positive (or negative) degrees, respectively. Bundle orientation of most IHCs and OHCs was −90° to +90°, with −30° to +30° regarded as normal (*SI Appendix*, Fig. S4*F*) (38). Stereociliary bundle orientation distribution histograms were generated from these measurements. The distribution of stereociliary bundle orientation was similar across all four genotypes (one-way ANOVA, *SI Appendix*, Fig. S4*G*). We also plotted and analyzed exact angle measurements for each individual OHC and IHC (*SI Appendix*, Fig. S4*H*). The distribution of stereociliary bundle orientation was similar across all four genotypes using the nonequal concentration parameter approach ANOVA test (39). These data suggest that neither *Chd7* nor *Sox2* are required for regulation of stereociliary bundle orientation. Double heterozygous loss of *Chd7* and *Sox2* leads to supernumerary IHCs and OHCs that appear to be innervated, associated with SCs, and exhibit normally formed and oriented stereociliary bundles.

RNA Sequencing and CUT&Tag Identify Putative CHD7 and SOX2 Target Genes and Genomic Binding Sites. Dynamic expression of *Chd7* and *Sox2* during inner ear development, combined with *Chd7* regulation of *Sox2* and robust inner ear phenotypes in double heterozygous mutant ears, led us to hypothesize that CHD7 and SOX2 may regulate downstream gene expression in potentially synergistic ways. To address this, we performed bulk RNA sequencing on E10.5 otocysts from all four genotypes (WT, $Chd7^{Gt/+}$, $Sox2^{CreER/+}$, and $Chd7^{Gt/+};Sox2^{CreER/+}$) (Fig. 5*A*). *Chd7* expression was down-regulated in $Chd7^{Gt/+}$ and $Chd7^{Gt/+};Sox2^{CreER/+}$ otocysts compared to WT (*SI Appendix*, Fig. S5*A*), and *Sox2* was down-regulated in $Chd7^{Gt/+};Sox2^{CreER/+}$ otocysts relative to WT, $Chd7^{Gt/+}$, or $Sox2^{CreER/+}$ otocysts (*SI Appendix*, Fig. S5*B*) (40). In contrast, *Sox2* was not down-regulated in $Chd7^{Gt/+}$ or $Sox2^{CreER/+}$ otocysts compared to WT (*SI Appendix*, Fig. S5*B*), suggesting that SOX2 autoregulates its own transcription even in the context of haploinsufficiency, as previously shown in other tissues and cell types. This result is also consistent with previous single-cell qPCR studies in $Chd7^{Gt/+}$ vs. WT E10.5 otocysts (41).

RNA sequencing revealed 63 differentially expressed genes (DEGs) in $Chd7^{Gt/+}$ otocysts compared to WT, including *Chd7* (*SI Appendix*, Fig. S5*C*). These DEGs included 45 down-regulated and 18 up-regulated genes, with relevant GO terms including sensory cell morphogenesis, neurogenesis, and epithelial cell development (*SI Appendix*, Fig. S5*E*). In contrast to *Chd7*, heterozygous loss of *Sox2* had minimal impact on the transcriptional landscape of the E10.5 otocyst, with only five genes differentially expressed between $Sox2^{CreER/+}$ and WT samples (*SI Appendix*, Fig. S5*D*). We identified 130 DEGs (55 up-regulated and 75 down-regulated) in $Chd7^{Gt/+};Sox2^{CreER/+}$ otocysts compared to WT, including *Chd7* and *Sox2* (Fig. 5*B*). This represents a twofold higher number of DEGs in $Chd7^{Gt/+};Sox2^{CreER/+}$compared to $Chd7^{Gt/+}$ otocysts (*SI Appendix*, Fig. S5*C*). GO term analysis of these 130 DEGs indicated biological processes including regulation of Smoothened and Notch signaling, sensory organ and nervous system morphogenesis, and cell fate commitment (Fig. 5*C*).

RNA sequencing showed several DEGs in E10.5 $Chd7^{Gt/+};Sox2^{CreER/+}$ otocysts that are known to specify the dorsal region and contribute to vestibular development including *Bmper* (41), *Wnt7b* (42), *Fgf3* (43), and *Fgf10* (44). We also found that *Aldh1a3* is up-regulated in $Chd7^{Gt/+};Sox2^{CreER/+}$ ears, which is consistent with a previous study showing that *Aldh1a3* is up-regulated in $Chd7^{Gt/+}$ and $Chd7^{Gt/Gt}$otocysts (45). Ventral specifying genes, including *Otx2* (46) and *Etv5* (47), were also differentially expressed in E10.5 $Chd7^{Gt/+};Sox2^{CreER/+}$ otocysts. Additional DEGs, including *Pax2* (48) and *Fgfr2* (49), are also known to be involved in both vestibular and cochlear morphogenesis, suggesting that changes in the expression of critical patterning genes contribute to the phenotypes observed with loss of *Chd7* and *Sox2*.

Since CHD7 and SOX2 physically interact in neural stem cells, we asked whether CHD7 and SOX2 bind to similar genomic regions during otic development. To identify CHD7 and SOX2 binding sites, we performed Cleavage Under Targets & Tagmentation (CUT&Tag) on WT otocysts microdissected from E10.5 embryos (Fig. 5*A*). Our CUT&Tag dataset, together with bulk RNA sequencing data, have been deposited into the NCBI Gene Expression Omnibus (GEO: GSE239363) database. Sparse Enrichment Analysis for CUT&RUN (SEACR) was employed to identify regions (peaks) that displayed statistically significant enrichment of CHD7 or SOX2. SEACR identified 33,035 CHD7 peaks and 155,548 SOX2 peaks from CUT&Tag libraries. Since we were interested in how CHD7 and SOX2 function together or individually, we identified three distinct types CUT&Tag reads based on occupancy by both CHD7 and SOX2 (21,403), CHD7 only (11,449) or SOX2 only (132,639) (Fig. 5*D*). Profile plots showed a similar distribution (*SI Appendix*, Fig. S6*A*). CHD7+SOX2+ sites were further examined to identify a common genetic network. Since CHD7 and SOX2 are known to bind cis-regulatory elements, we determined whether CHD7+SOX2+ signals were present in regions near TSSs or enhancers. As expected, heatmaps of CHD7+SOX2+ regions near TSSs and enhancers showed both CUT&Tag CHD7 and SOX2 signals (Fig. 5*E*). Profile plots also confirmed the distribution at these sites (*SI Appendix*, Fig. S6*B*). We found 4,968 CHD7+SOX2+ sites associated with TSSs and 5,822 CHD7+SOX2+ sites associated with enhancers (Fig. 5*F*). Thus, the majority of the CHD7/SOX2 bound sites may correspond to cis-regulatory regions away from TSSs or enhancers that are yet to be defined. We then used HOMER to identify enriched motifs at CHD7+SOX2+ genomic regions (50). The known SOX2 motif ($P < 1 \times 10^{-7}$) (Fig. 5*G*) in 2.81% of the CHD7+SOX2+ sites contained a consensus

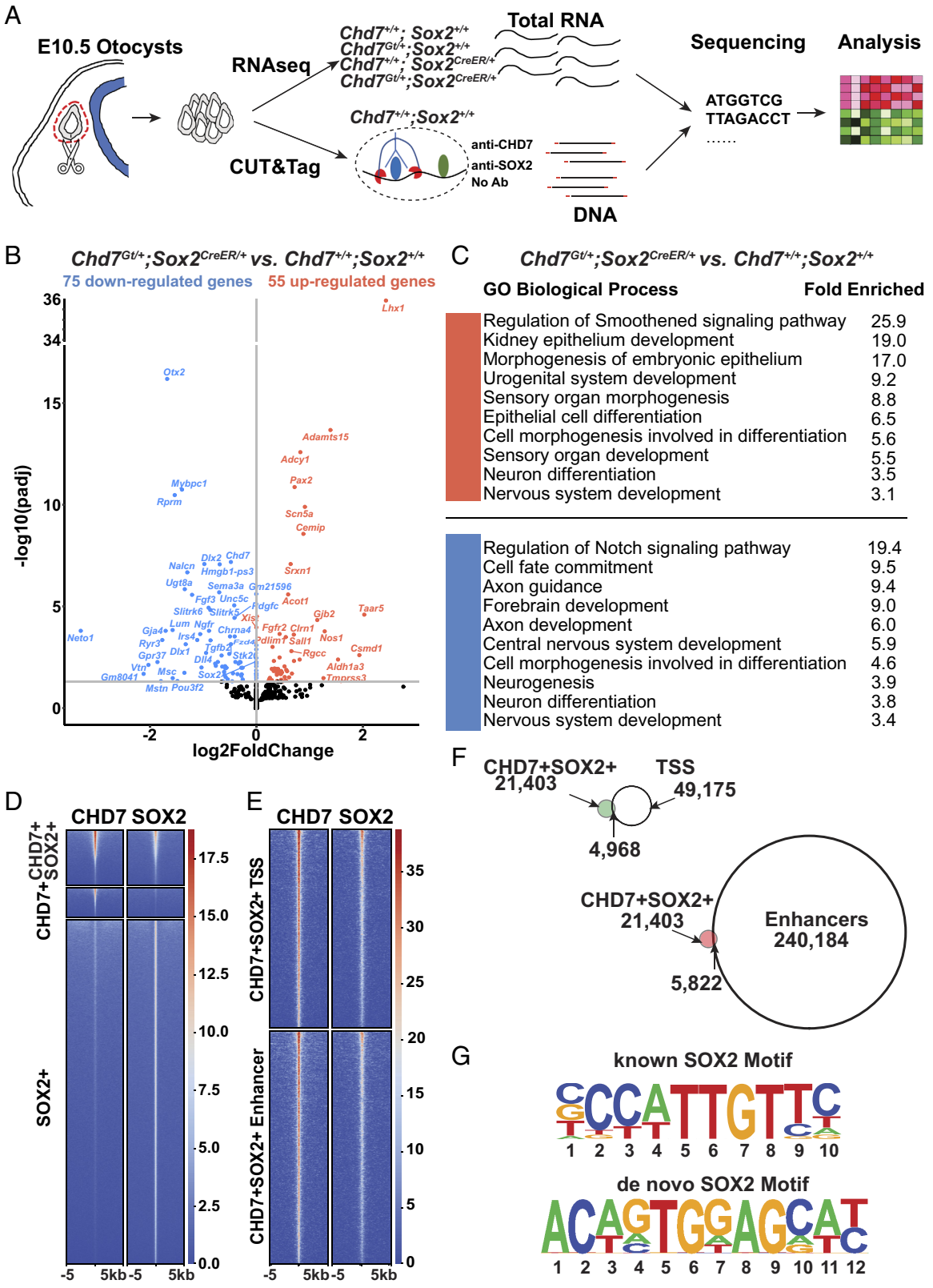

Fig. 5. RNA sequencing and CUT&Tag identify putative CHD7 and SOX2 target genes and genomic binding sites. (*A*) Multiomic approach using bulk RNA sequencing and CUT&Tag on microdissected E10.5 otocysts. (*B*) Volcano plot of DEGs in *Chd7*$^{Gt/+}$;*Sox2*$^{CreER/+}$ vs. WT ears. Unaffected genes are shown in black, down-regulated genes in blue and up-regulated genes in red. *Sox2* was down-regulated in *Chd7*$^{Gt/+}$;*Sox2*$^{CreER/+}$ ears. (*C*) Table showing *Top* enriched GO terms among up-regulated (red) and down-regulated (blue) genes in *Chd7*$^{Gt/+}$;*Sox2*$^{CreER/+}$ vs. WT otocysts. (*D*) Identification of CHD7 and SOX2 target genomic regions by CUT&Tag in WT otocysts. Bedtools was used to define three categories, CHD7+SOX2+, CHD7+, and SOX2+, based on CHD7 and SOX2 occupancy. Heatmaps of CHD7 and SOX2 CUT&Tag signal centered at 21,403 CHD7+SOX2+, 11,449 CHD7+ and 132,639 SOX2+ genomic regions. (*E*) CHD7+SOX2+ regions associated with TSS or ENCODE-defined enhancers. Heatmaps of CHD7 and SOX2 CUT&Tag signals at 4,968 CHD7+SOX2+ TSS or 5,822 CHD7+SOX2+ enhancer regions. Heatmap signals centered ±5 kb around the summit of SEACR-defined peaks and represented as reads per kilobase per million (RPKM). (*F*) Venn diagrams display the intersection between CHD7+SOX2+ peaks at TSS or enhancer regions and show 4,968 CHD7+SOX2+ TSS and 5,822 CHD7+SOX2+ enhancers. (*G*) Differential motif discovery using HOMER revealed known SOX2 ($P = 1 \times 10^{-7}$) and de novo SOX2 ($P = 1 \times 10^{-49}$) motifs using a nonspecific control CUT&Tag as background.

sequence bound by the high mobility group binding domain of SOX2 (ATTGTT) (51), which was previously confirmed by large-scale transcription factor binding analysis (52). De novo motif analysis also identified a SOX2 binding site in 0.32% of the CHD7+SOX2+ binding sites ($P < 1 \times 10^{-49}$) which contained a sequence (ACAATG) identified using in vitro binding assays (Fig. 5*G*) (53). CHD7 contains a DNA binding domain (54) but no known consensus DNA binding site, suggesting that its binding is context dependent. Motif analysis confirmed that some CHD7+SOX2+ genomic regions harbor SOX2 motifs. These known and de novo motifs represent a small fraction of identified CHD7+SOX2+ sequences with SOX2 consensus binding sites and likely reflect the influence of CHD7 activity or the requirement for SOX2 to cooperatively partner with other DNA binding factors (55). Together, these results help to describe a CHD7 and SOX2 gene regulatory network in E10.5 otic cells.

Integrative Analysis Identifies Common CHD7 and SOX2 Regulators of Inner Ear Development. To gain further insight into genes directly regulated by CHD7 and SOX2, we filtered candidate DEGs based on CHD7 and SOX2 CUT&Tag signals within ±5 kb of TSSs or within enhancers. Of the 75 genes down-regulated in $Chd7^{Gt/+};Sox2^{CreER/+}$ otocysts, 49 were cobound by CHD7 and SOX2, and 35 of these were cobound by CHD7 and SOX2 near their TSSs and/or in enhancers. Eleven of these genes are known to be expressed in the otocyst, and three (*Otx2, Sox2, and Dusp6*) are associated with human hearing loss (Fig. 6*A*). Of the 55 genes up-regulated in $Chd7^{Gt/+};Sox2^{CreER/+}$, 27 were cobound by CHD7 and SOX2, and among these, 23 were cobound by CHD7 and SOX2 near their TSSs and/or in enhancers. Thirteen of these genes have reported expression in the otocyst, and three (*Pax2, Fgfr2,* and *Sall1*) are associated with human hearing loss (Fig. 6*A*). Gene ontology (GO) analysis using Database for Annotation, Visualization, and Integrated Discovery (DAVID) was performed on the 49 down-regulated genes and 27 up-regulated genes, revealing biological processes such as ear development and morphogenesis (*SI Appendix*, Fig. S6*C*). To further investigate binding of CHD7 and SOX2 at these genes, genomic tracks of target genes were visualized. No CHD7 and SOX2 protein enrichment were found within ±5 kb of the *Chd7* TSS. However, enrichment was observed in the first intron of *Chd7* (Fig. 6*B*), a region consistent for the location of a distal enhancer. Enrichment of CHD7 and SOX2 proteins around *Sox2* TSS is consistent with autoregulation of *Sox2* gene expression in otic cell types (Fig. 6*C*). CHD7 and SOX2 enrichment near the TSSs of *Pax2* and *Otx2* also suggest direct regulation (Fig. 6 *D* and *E*). We confirmed *Pax2* and *Otx2* expression dysregulation by comparing immunofluorescence in double heterozygous otocysts relative to WT (Fig. 6*F*). The mean immunofluorescence intensity of PAX2 staining in doubly heterozygous ears ($n = 6$ ears) was 20% higher than in WT ears ($n = 4$ ears, $P < 0.05$, unpaired t test). The percentage of OTX2+ positive region in double heterozygous otocysts ($n = 6$ ears) was reduced 83.3% compared to WT ears ($n = 6$ ears, $P < 0.01$, unpaired t test). CHD7 and SOX2 proteins were also enriched near the TSSs of other genes involved in human deafness (*Dusp6*, *Fgfr2,* and *Sall1*) and known to be expressed in the E10.5 otocyst (*Etv1*, *Irx3,* and *Shisa2*) (*SI Appendix*, Fig. S7*A*). CHD7 and SOX2 proteins are also enriched at the enhancers of some genes including *Fgf10* and *Aldh1a3* (*SI Appendix*, Fig. S7*B*). Taken together, these results suggest that CHD7 and SOX2 establish a regulatory network during early otic development that includes *Pax2*, *Otx2,* and other critical genes.

Discussion

In this study, we found that *Chd7* and *Sox2* are expressed in the developing mammalian inner ear in a highly dynamic manner, with extensive colocalization in the E10.5 otocyst and subsequent segregation of the two proteins in both HCs and SCs (CHD7) vs. SCs (SOX2). We also uncovered unique phenotypes related to *Chd7* and/or *Sox2* deficiency in the developing vestibular and auditory portions of the inner ear. Double *Chd7*;*Sox2* heterozygotes showed severe hypoplasia of all three semicircular canals and cochlea, likely related to reduced cell proliferation in the developing otocyst. Double *Chd7*;*Sox2* heterozygotes also exhibited supernumerary cochlear HCs, normal stereociliary bundle orientation, and innervation. A critical developmental period (~E9.5) of increased sensitivity to combined *Chd7* and *Sox2* loss was determined using conditional and inducible loss of *Chd7* by $Sox2^{CreER}$. Genome-wide expression and DNA binding assays identified several candidate target genes for *Chd7* and *Sox2* in the otocyst, including the early otic patterning genes *Otx2* and *Pax2*. A model (Fig. 6*H*) of our findings depicts CHD7 and SOX2 binding near the TSSs or enhancers to promote expression of genes including *Sox2, Otx2,* and *Dusp6* and inhibit expression of *Pax2*, *Fgfr2, and Sall1,* among others.

These studies shed light on roles for *Chd7* and *Sox2* in vestibular and cochlear morphogenesis, summarized in Fig. 6*G*. Normal semicircular canal formation relies on correct dosage of both *Chd7* and *Sox2*. Loss of one *Chd7* allele in $Chd7^{Gt/+}$ mice results in abnormal lateral and posterior semicircular canals (25, 27), while loss of both *Chd7* alleles in *Chd7* conditional nulls (using *Pax2Cre* or $Foxg1^{Cre/+}$) leads to severe hypoplasia of anterior, posterior, and lateral semicircular canals (10, 13). Loss of a single *Sox2* allele is associated with normal vestibular development, while loss of both Sox2 alleles in *Lcc/Lcc* mutants leads to severely hypoplastic semicircular canals and cochleae (17). In the current study, we found that loss of one copy each of *Chd7* and *Sox2* results in inner ear abnormalities that resemble those observed in mice with loss of both alleles of *Chd7* or *Sox2*. Previous reports also showed hypoplastic cochleae in *Chd7* conditional knock-out mice using either $Foxg1^{Cre/+}$ (10) or *Pax2Cre* (13), and in mice with inner ear-specific deletion of *Sox2* prior to E10.5 (21) or loss of *Sox2* in *Lcc/Lcc* mutants (17). Neither $Chd7^{Gt/+}$ nor $Sox2^{CreER/+}$ mice exhibited shortened cochleae or cochlear cellular abnormalities beyond the supernumerary IHCs in $Sox2^{CreER/+}$ mice. However, $Chd7^{Gt/+};Sox2^{CreER/+}$ embryos exhibited shortened cochlea and supernumerary OHCs and IHCs. Taken together, these results show that combined loss of *Chd7* and *Sox2* genes is detrimental to both cochlear and vestibular morphogenesis.

The results from our study may help distinguish among four distinct mechanisms regulating development of cochlear structures: cellular growth, cell proliferation, convergent extension, and radial intercalation. Beginning around E11 in the mouse, most cell types that line the cochlear duct continue to proliferate throughout at least early postnatal stages such that addition of new cells contributes to cochlear outgrowth (1, 6). Beyond E16, physical growth of HCs also contributes to continued cochlear extension (1, 6). We observed no obvious differences in HC size between WT and $Chd7^{Gt/+};Sox2^{CreER/+}$ cochleae. In contrast, we observed decreases in cell proliferation in the $Chd7^{Gt/+};Sox2^{CreER/+}$ E10.5 otocyst and E11.5 cochlear primordium that likely contribute to the shortened cochlea, especially since there was no concomitant increase in cell death or major alteration in the rate of progenitor CCE. In addition to cellular growth and proliferation, convergent extension and radial intercalation are key mechanisms that help transform the cochlea from a dense, pseudostratified epithelium to a bilayered structure, in which HCs locate luminally and SCs span the basal-luminal axis. Multiple signaling

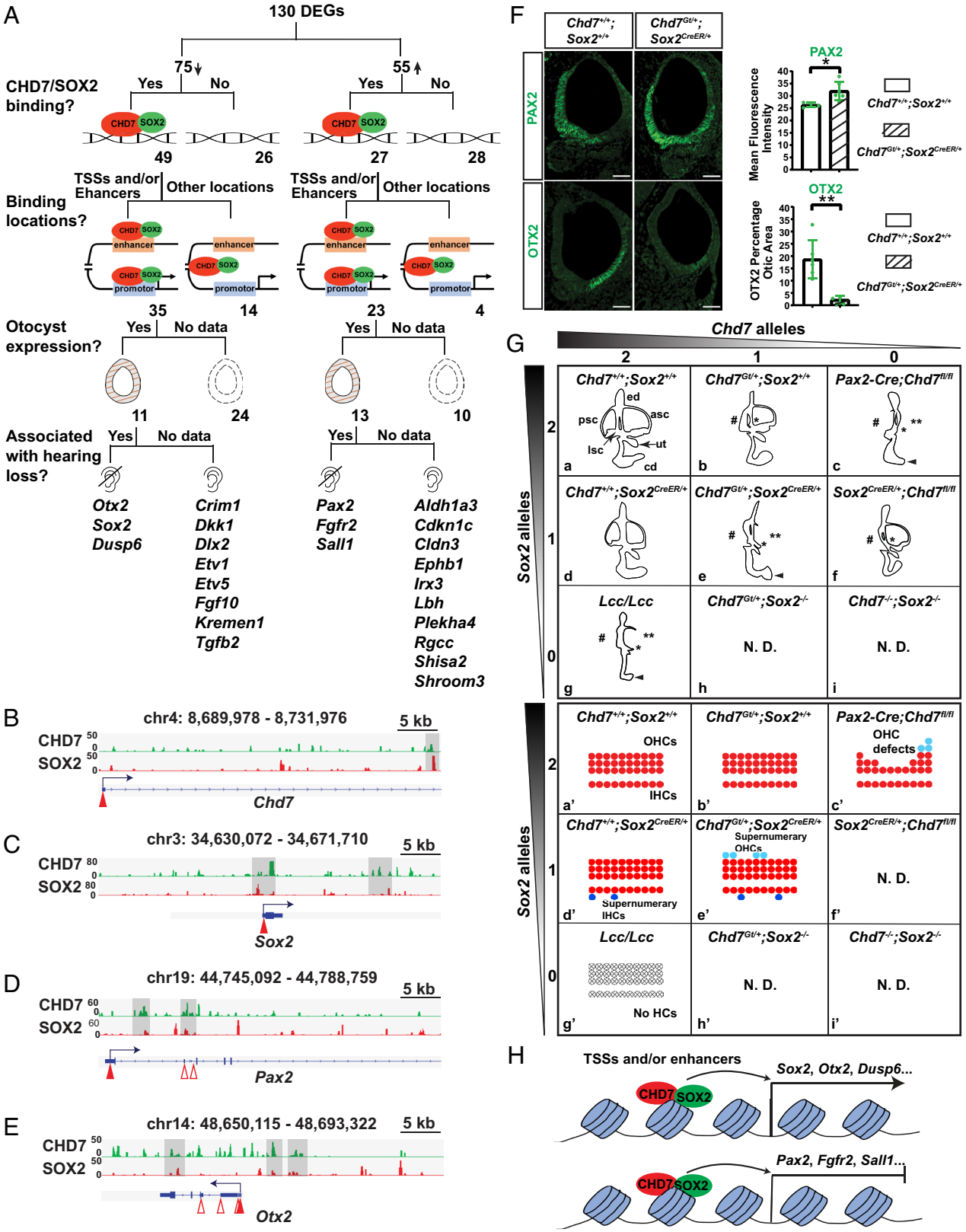

Fig. 6. Integrative analysis identifies common CHD7 and SOX2 regulators of inner ear development. (*A*) Integration of RNA sequencing and CUT&Tag results based on analyzing 130 DEGs with a series of criteria listed on the *Left*. The number of DEGs are shown after each filtering step. Down-regulated genes *Otx2*, *Sox2*, and *Dusp6* and up-regulated genes *Pax2, Fgfr2,* and *Sall1* meet all filtering criteria. (*B–E*) Genomic tracks of CHD7 and SOX2 CUT&Tag signals at the specified genomic coordinates of *Chd7*, *Sox2*, *Pax2*, and *Otx2* genes. Highlighted regions mark overlapping CHD7 and SOX2 peaks. Closed red arrowheads indicate the canonical TSS of the specified gene, and open red arrowheads indicate the alternative TSS. (*F*) Immunofluorescence of PAX2 and OTX2 in E10.5 otocysts from WT and *Chd7*$^{Gt/+}$;*Sox2*$^{CreER/+}$ double heterozygous embryos with quantification of PAX2 and OTX2 staining. (*G*) Cartoon showing inner ear and cochlear sensory epithelial defects associated with various dosages of *Chd7* and *Sox2* alleles. (*H*) Model showing how *Chd7* and *Sox2* cooperate to regulate gene expression during inner ear development. CHD7 and SOX2 form a complex, bind near TSSs and/or enhancers, and promote expression of *Sox2*, *Otx2*, *Dusp6,* and other genes. CHD7 and SOX2 can also repress expression of *Fgfr2*, *Pax2*, *Sall1*, and other genes in the developing otocyst. In (*G*), * indicates lateral semicircular canal defects; ** indicates anterior semicircular canal; # indicates posterior semicircular canal defects; arrowheads show shortened cochleae. Red dots represent normal OHCs and IHCs. Light and dark blue dots represent supernumerary OHCs and supernumerary IHCs, respectively. Dashed line circles with crosses in panel *Gg'* represent loss of all HCs. N.D. = not determined. [Scale bar in (*F*), 50 μm.]

pathways, including *Shh*, *Wnt*, and core PCP are involved in these aspects of cochlear outgrowth (1, 6). Our RNA sequencing in E10.5 $Chd7^{Gt/+};Sox2^{CreER/+}$ otocysts uncovered several DEGs which are components of *Shh* signaling (*Gli1*) or *Wnt* signaling (*Wnt7b* and *Fzd4*). These DEGs might account for the abnormal cochlear outgrowth in $Chd7^{Gt/+};Sox2^{CreER/+}$mice, but additional studies at later time points during cochlear development are necessary to clarify their precise spatiotemporal requirements. Mutations in some PCP pathway genes, for example, *Vangl2*, lead to shortened cochleae and abnormal stereociliary bundle orientation (38), and it will be interesting to determine whether PCP is also dependent upon *Chd7* and/or *Sox2*. Early insights into this question suggest that PCP pathways may be resistant to *Chd7*|*Sox2* loss since stereociliary bundle orientation was unchanged in the early postnatal $Chd7^{Gt/+};Sox2^{CreER/+}$ cochlea. Taken together, our results suggest that *Chd7* and *Sox2* control neurosensory progenitor proliferation and regulate expression of signaling pathway components involved in convergent extension and radial intercalation, but may be less important for cellular growth.

Our RNA sequencing and CUT&Tag results revealed several DEGs in the $Chd7^{Gt/+};Sox2^{CreER/+}$ E10.5 otocyst that were also cobound by CHD7 and SOX2 near their TSSs and/or enhancers. Several of these genes are critical for cochlear outgrowth and sensory progenitor differentiation, including *Pax2* (48), *Otx2* (46), *Etv5* (47), *Sall1* (56), and *Kremen1* (57). These gene expression changes, among others, may help explain the shortened cochlea and supernumerary HCs in $Chd7^{Gt/+};Sox2^{CreER/+}$ cochleae, which exhibit increased supernumerary HCs and SCs. The Notch signaling pathway seems less likely to be involved in $Chd7^{Gt/+};Sox2^{CreER/+}$ supernumerary OHC formation, since Notch mutants exhibit supernumerary HCs with concomitant reductions in SCs (36, 58). Our RNA sequencing also revealed dysregulation of some extracellular matrix (ECM) genes, such as *Adamts15*, which is expressed in the adult rat cochlea (59). Future studies will help determine whether *Adamts15* or other ECM genes are involved in generating these cochlear phenotypes.

Our studies provide evidence that *Chd7* acts upstream of and cooperatively with *Sox2* in a dosage-sensitive manner during a critical period of inner ear development. $Sox2^{CreER}$ mediated loss of both *Chd7* alleles at E8.5, E9.5, or E10.5 resulted in malformed E14.5 lateral and posterior semicircular canals that were most penetrant after tamoxifen treatment at E9.5. In contrast, $Sox2^{CreER}$ mediated loss of only one *Chd7* allele resulted in canal defects after tamoxifen administration at E9.5, but not at E8.5 or E10.5. These differences in conditional heterozygous inner ear phenotypes that occur after deleting one copy of *Chd7* on E8.5 vs. E9.5 may reflect dynamic changes in the expression of *Sox2* compared to *Chd7*, or differences in the timing of *Chd7*/*Sox2* genetic interactions. *Sox2* expression in the E8.5 lateral otocyst starts to decline at E9.5 and shifts to medial and ventral expression at E10.5 (20, 21). Since *Chd7* otic expression is broader than *Sox2* throughout E8.5-E10.5, (Fig. 1), there may be sufficient *Chd7* WT otic cells remaining in E8.5 tamoxifen-treated $Sox2Cre^{ER};Chd7^{flox/+}$ mice to allow for normal inner ear development. Alternatively, the inner ear may be most sensitive to combined *Chd7* and *Sox2* loss around E9.5. Future experiments tracking the fates of *Chd7* lineage cells will help distinguish among these possibilities.

The chromatin remodeling activity of CHD7, combined with evidence that SOX2 acts as a pioneer transcription factor (60), raises the possibility that these two proteins mediate changes in chromatin architecture by influencing the levels and timing of target gene expression. Together, these results support a gene regulatory network involving an important chromatin remodeling factor and a key transcription factor during inner ear morphogenesis. Genetic interactions between *Chd7* and *Sox2* may also have implications for human genetic disorders. Autosomal dominant pathogenic variants in human *CHD7* are the major cause of CHARGE syndrome, and pathogenic variants in human *SOX2* lead to microphthalmia. The pattern of malformations and clinical features varies greatly among individuals with CHARGE syndrome and with *SOX2*-related microphthalmia, even among members of the same family with the same sequence variant (61, 62). This phenotypic variability could also be related to the consequences of modifier genes that alter the penetrance and expressivity of certain clinical features. As an example of modifier gene activity, nonsyndromic autosomal recessive deafness-12 (DFNB12) is caused by homozygous or compound heterozygous pathogenic variants in the Cadherin-23 gene, and a variant in the *ATP2B2* gene modifies the severity of sensorineural hearing loss (63). Further investigations using emerging genomic data on individuals with syndromic vestibular and/or hearing losses will help clarify whether *SOX2* and *CHD7* can also act as modifier genes to promote early mammalian vestibular and auditory development.

Materials and Methods

The following mouse strains were used in this study (with their Jackson Laboratory identification numbers): $Chd7^{Gt/+}$ (030659), $Chd7^{flox/flox}$ (030660), $Sox2^{CreER/+}$ (017593), and $Sox2^{flox/flox}$ (013093). $Chd7^{Gt/+}$ and $Sox2^{CreER/+}$ mice were maintained by backcrossing with B6129SF1/J mice (101043). $Chd7^{flox/flox}$ mice were maintained on a mixed C57BL/6;129S1/SvImJ background. All procedures were approved by The University of Michigan Institutional Animal Care & Use Committee.

Details on *Cre* induction, immunofluorescence, paint-fills, EdU injection, RNA sequencing, and CUT&Tag are provided in *SI Appendix, SI Materials and Methods*.

Sequencing datasets for RNA sequencing and CUT&Tag were deposited into the NCBI GEO (GSE239363) database.

Data, Materials, and Software Availability. The data reported in this paper have been deposited in the GEO database, https://www.ncbi.nlm.nih.gov/geo (accession no. GSE239363) (64).

ACKNOWLEDGMENTS. Y.R., K.Y.K., and D.M.M. are supported by NIH R01DC018404. Y.R. is supported by the R. Jamison and Betty Williams Professor of Otolaryngology. D.M.M. is supported by the Taubman Medical Institute and the Ravitz Foundation Professorship in Pediatrics. K.E.R. was supported by NIH T32 DC000011.

Author affiliations: [a]Department of Pediatrics, The University of Michigan, Ann Arbor, MI 48109; [b]Department of Cell Biology and Neuroscience, Rutgers University, Piscataway, NJ 08854; [c]Keck Center for Collaborative Neuroscience, Stem Cell Research Center, Rutgers University, Piscataway, NJ 08854; [d]Medical Scientist Training Program, The University of Michigan, Ann Arbor, MI 48109; [e]Department of Otolaryngology-Head and Neck Surgery, The University of Michigan, Ann Arbor, MI 48109; and [f]Department of Human Genetics, The University of Michigan, Ann Arbor, MI 48109

1. E. C. Driver, M. W. Kelley, Development of the cochlea. *Development* **147**, dev162263 (2020).
2. J. Bok, W. Chang, D. K. Wu, Patterning and morphogenesis of the vertebrate inner ear. *Int. J. Dev. Biol.* **51**, 521–533 (2007).
3. A. K. Groves, D. M. Fekete, Shaping sound in space: The regulation of inner ear patterning. *Development* **139**, 245–257 (2012).
4. D. K. Wu, M. W. Kelley, Molecular mechanisms of inner ear development. *Cold Spring Harb. Perspect. Biol.* **4**, a008409 (2012).
5. H. Gálvez, G. Abelló, F. Giraldez, Signaling and transcription factors during inner ear development: The generation of hair cells and otic neurons. *Front. Cell Dev. Biol.* **5**, 21 (2017).
6. M. Montcouquiol, M. W. Kelley, Development and patterning of the cochlea: From convergent extension to planar polarity. *Cold Spring Harb. Perspect. Med.* **10**, a033266 (2020).
7. E. A. Bosman *et al.*, Multiple mutations in mouse Chd7 provide models for CHARGE syndrome. *Hum. Mol. Genet.* **14**, 3463–3476 (2005).

8. L. E. Vissers *et al.*, Mutations in a new member of the chromodomain gene family cause CHARGE syndrome. *Nat. Genet.* **36**, 955–957 (2004).
9. M. E. Adams *et al.*, Defects in vestibular sensory epithelia and innervation in mice with loss of Chd7 function: Implications for human CHARGE syndrome. *J. Comp. Neurol.* **504**, 519–532 (2007).
10. E. A. Hurd, H. K. Poucher, K. Cheng, Y. Raphael, D. M. Martin, The ATP-dependent chromatin remodeling enzyme CHD7 regulates pro-neural gene expression and neurogenesis in the inner ear. *Development* **137**, 3139–3150 (2010).
11. E. A. Hurd *et al.*, Mature middle and inner ears express Chd7 and exhibit distinctive pathologies in a mouse model of CHARGE syndrome. *Hear Res.* **282**, 184–195 (2011).
12. K. E. Ritter *et al.*, Loss of the chromatin remodeler CHD7 impacts glial cells and myelination in the mouse cochlear spiral ganglion. *Hear. Res.* **426**, 108633 (2022).
13. V. Balendran *et al.*, Chromatin remodeler CHD7 is critical for cochlear morphogenesis and neurosensory patterning. *Dev. Biol.* **477**, 11–21 (2021).
14. K. S. E. Cheah, P.-X. Xu, "Chapter 15–SOX2 in neurosensory fate determination and differentiation in the inner ear" in *Sox2*, H. Kondoh, R. Lovell-Badge, Eds. (Academic Press, Boston, 2016), pp. 263–280, https://doi.org/10.1016/B978-0-12-800352-7.00015-3.
15. A. C. Mak, I. Y. Szeto, B. Fritzsch, K. S. Cheah, Differential and overlapping expression pattern of SOX2 and SOX9 in inner ear development. *Gene Expr. Patterns* **9**, 444–453 (2009).
16. J. Neves, I. Vachkov, F. Giraldez, Sox2 regulation of hair cell development: Incoherence makes sense. *Hear. Res.* **297**, 20–29 (2013).
17. A. E. Kiernan *et al.*, Sox2 is required for sensory organ development in the mammalian inner ear. *Nature* **434**, 1031–1035 (2005).
18. J. S. Kempfle, J. L. Turban, A. S. Edge, Sox2 in the differentiation of cochlear progenitor cells. *Sci. Rep.* **6**, 23293 (2016).
19. A. R. Steevens, D. L. Sookiasian, J. C. Glatzer, A. E. Kiernan, SOX2 is required for inner ear neurogenesis. *Sci. Rep.* **7**, 4086 (2017).
20. R. Gu *et al.*, Lineage tracing of Sox2-expressing progenitor cells in the mouse inner ear reveals a broad contribution to non-sensory tissues and insights into the origin of the organ of Corti. *Dev. Biol.* **414**, 72–84 (2016).
21. A. R. Steevens *et al.*, SOX2 is required for inner ear growth and cochlear nonsensory formation before sensory development. *Development* **146**, dev170522 (2019).
22. M. P. Schnetz *et al.*, CHD7 targets active gene enhancer elements to modulate ES cell-specific gene expression. *PLoS Genet.* **6**, e1001023 (2010).
23. E. Engelen *et al.*, Sox2 cooperates with Chd7 to regulate genes that are mutated in human syndromes. *Nat. Genet.* **43**, 607–611 (2011).
24. T. Doi *et al.*, Chd7 collaborates with Sox2 to regulate activation of oligodendrocyte precursor cells after spinal cord injury. *J. Neurosci.* **37**, 10290–10309 (2017).
25. E. A. Hurd, J. A. Micucci, E. N. Reamer, D. M. Martin, Delayed fusion and altered gene expression contribute to semicircular canal defects in Chd7 deficient mice. *Mech. Dev.* **129**, 308–323 (2012).
26. V. Randall *et al.*, Great vessel development requires biallelic expression of Chd7 and Tbx1 in pharyngeal ectoderm in mice. *J. Clin. Invest.* **119**, 3301–3310 (2009).
27. E. A. Hurd *et al.*, Loss of Chd7 function in gene-trapped reporter mice is embryonic lethal and associated with severe defects in multiple developing tissues. *Mamm. Genome* **18**, 94–104 (2007).
28. A. A. Avilion *et al.*, Multipotent cell lineages in early mouse development depend on SOX2 function. *Genes Dev.* **17**, 126–140 (2003).
29. K. Arnold *et al.*, Sox2(+) adult stem and progenitor cells are important for tissue regeneration and survival of mice. *Cell Stem Cell* **9**, 317–329 (2011).
30. P. J. Atkinson *et al.*, Sox2 haploinsufficiency primes regeneration and Wnt responsiveness in the mouse cochlea. *J. Clin. Invest.* **128**, 1641–1656 (2018).
31. M. Kaiser *et al.*, Regulation of otocyst patterning by Tbx2 and Tbx3 is required for inner ear morphogenesis in the mouse. *Development* **148**, dev195651 (2021).
32. J. Bok, C. Zenczak, C. H. Hwang, D. K. Wu, Auditory ganglion source of Sonic hedgehog regulates timing of cell cycle exit and differentiation of mammalian cochlear hair cells. *Proc. Natl. Acad. Sci. U.S.A.* **110**, 13869–13874 (2013).
33. C. R. Hume, D. L. Bratt, E. C. Oesterle, Expression of LHX3 and SOX2 during mouse inner ear development. *Gene Expr. Patterns* **7**, 798–807 (2007).
34. A. Dabdoub *et al.*, Sox2 signaling in prosensory domain specification and subsequent hair cell differentiation in the developing cochlea. *Proc. Natl. Acad. Sci. U.S.A.* **105**, 18396–18401 (2008).
35. L. Delacroix, B. Malgrange, Cochlear afferent innervation development. *Hear. Res.* **330**, 157–169 (2015).
36. A. E. Kiernan, R. Cordes, R. Kopan, A. Gossler, T. Gridley, The Notch ligands DLL1 and JAG2 act synergistically to regulate hair cell development in the mammalian inner ear. *Development* **132**, 4353–4362 (2005).
37. O. Bermingham-McDonogh *et al.*, Expression of Prox1 during mouse cochlear development. *J. Comp. Neurol.* **496**, 172–186 (2006).
38. M. Montcouquiol *et al.*, Identification of Vangl2 and Scrb1 as planar polarity genes in mammals. *Nature* **423**, 173–177 (2003).
39. L. Landler, G. D. Ruxton, E. P. Malkemper, Advice on comparing two independent samples of circular data in biology. *Sci. Rep.* **11**, 20337 (2021).
40. T. Schaefer, C. Lengerke, SOX2 protein biochemistry in stemness, reprogramming, and cancer: The PI3K/AKT/SOX2 axis and beyond. *Oncogene* **39**, 278–292 (2020).
41. R. Durruthy-Durruthy *et al.*, Single cell transcriptomics reveal abnormalities in neurosensory patterning of the Chd7 mutant mouse ear. *Front. Genet.* **9**, 473 (2018).
42. R. Yamamoto, H. Ohnishi, K. Omori, N. Yamamoto, In silico analysis of inner ear development using public whole embryonic body single-cell RNA-sequencing data. *Dev. Biol.* **469**, 160–171 (2021).
43. E. P. Hatch, C. A. Noyes, X. Wang, T. J. Wright, S. L. Mansour, Fgf3 is required for dorsal patterning and morphogenesis of the inner ear epithelium. *Development* **134**, 3615–3625 (2007).
44. S. Pauley *et al.*, Expression and function of FGF10 in mammalian inner ear development. *Dev. Dyn.* **227**, 203–215 (2003).
45. H. Yao *et al.*, CHD7 represses the retinoic acid synthesis enzyme ALDH1A3 during inner ear development. *JCI Insight* **3**, e97440 (2018).
46. V. Vendrell *et al.*, Otx2 is a target of N-myc and acts as a suppressor of sensory development in the mammalian cochlea. *Development* **142**, 2792–2800 (2015).
47. M. Ebeid, S. H. Huh, Mesenchymal ETV transcription factors regulate cochlear length. *Hear. Res.* **396**, 108039 (2020).
48. Q. Burton, L. K. Cole, M. Mulheisen, W. Chang, D. K. Wu, The role of Pax2 in mouse inner ear development. *Dev. Biol.* **272**, 161–175 (2004).
49. U. Pirvola *et al.*, FGF/FGFR-2(IIIb) signaling is essential for inner ear morphogenesis. *J. Neurosci.* **20**, 6125–6134 (2000).
50. S. Heinz *et al.*, Simple combinations of lineage-determining transcription factors prime cis-regulatory elements required for macrophage and B cell identities. *Mol. Cell* **38**, 576–589 (2010).
51. G. Badis *et al.*, Diversity and complexity in DNA recognition by transcription factors. *Science* **324**, 1720–1723 (2009).
52. C. Jia, M. B. Carson, Y. Wang, Y. Lin, H. Lu, A new exhaustive method and strategy for finding motifs in ChIP-enriched regions. *PLoS One* **9**, e86044 (2014).
53. M. Maruyama, T. Ichisaka, M. Nakagawa, S. Yamanaka, Differential roles for Sox15 and Sox2 in transcriptional control in mouse embryonic stem cells. *J. Biol. Chem.* **280**, 24371–24379 (2005).
54. B. J. Manning, T. Yusufzai, The ATP-dependent chromatin remodeling enzymes CHD6, CHD7, and CHD8 exhibit distinct nucleosome binding and remodeling activities. *J. Biol. Chem.* **292**, 11927–11936 (2017).
55. H. Kondoh, Y. Kamachi, SOX-partner code for cell specification: Regulatory target selection and underlying molecular mechanisms. *Int. J. Biochem. Cell Biol.* **42**, 391–399 (2010).
56. L. M. Yang, L. Stout, M. Rauchman, D. M. Ornitz, Analysis of FGF20-regulated genes in organ of Corti progenitors by translating ribosome affinity purification. *Dev. Dyn.* **249**, 1217–1242 (2020).
57. J. F. Mulvaney *et al.*, Kremen1 regulates mechanosensory hair cell development in the mammalian cochlea and the zebrafish lateral line. *Sci. Rep.* **6**, 31668 (2016).
58. C. Haddon, Y. J. Jiang, L. Smithers, J. Lewis, Delta-Notch signalling and the patterning of sensory cell differentiation in the zebrafish ear: Evidence from the mind bomb mutant. *Development* **125**, 4637–4644 (1998).
59. B. H. Hu *et al.*, Metalloproteinases and their associated genes contribute to the functional integrity and noise-induced damage in the cochlear sensory epithelium. *J. Neurosci.* **32**, 14927–14941 (2012).
60. S. O. Dodonova, F. Zhu, C. Dienemann, J. Taipale, P. Cramer, Nucleosome-bound SOX2 and SOX11 structures elucidate pioneer factor function. *Nature* **580**, 669–672 (2020).
61. M. C. Jongmans *et al.*, Familial CHARGE syndrome and the CHD7 gene: A recurrent missense mutation, intrafamilial recurrence and variability. *Am. J. Med. Genet. A* **146A**, 43–50 (2008).
62. J. C. Zenteno, H. J. Perez-Cano, M. Aguinaga, Anophthalmia-esophageal atresia syndrome caused by an SOX2 gene deletion in monozygotic twin brothers with markedly discordant phenotypes. *Am. J. Med. Genet. A* **140**, 1899–1903 (2006).
63. K. Rahit, M. Tarailo-Graovac, Genetic modifiers and rare Mendelian disease. *Genes (Basel)* **11**, 239 (2020).
64. J. Gao *et al.*, CHD7 and SOX2 Act in a Common Gene Regulatory Network During Mammalian Semicircular Canal and Cochlear Development. GEO. https://www.ncbi.nlm.nih.gov/geo/query/acc.cgi?acc=GSE239363. Deposited 26 July 2023.